Orientation of doubly excited states in N₂

John E. Furst

School of Mathematical and Physical Sciences, University of Newcastle, Ourimbah 2258, New South Wales, Australia

T. J. Gay and Joshua Machacek

Jorgensen Hall, University of Nebraska, Lincoln, Nebraska 68588-0299, USA

David Kilkoyne

Lawrence Berkeley National Laboratory, Berkeley, California 94720, USA

Kenneth W. McLaughlin

Department of Physics and Engineering, Loras College, Dubuque, Iowa 52001, USA

We have measured the total fluorescent intensity and circular polarization of light emitted in $3p\,^4P^o \to 3s\,^4P$ transitions of excited neutral nitrogen atoms created by the photofragmentation of the N_2 molecule with circularly polarized light having energies between 21 and 26 eV. The intensity measurements show the effect of predissociation of the N_2 Rydberg series $R(C)\,^1\Sigma_u^+$ states by non-Rydberg doubly excited resonances (NRDERs), while nonzero values of circular polarization allow us to unambiguously identify the presence of a directly excited NRDER with $^1\Pi_u$ symmetry in this energy range.

The interaction of light with diatomic molecules causing dissociation is perhaps the simplest chemical reaction. However, the dynamics of dissociation processes involving superexcited [1] or doubly excited states are not well understood. Such states are interesting because they provide good examples of energetic but highly correlated systems. While these doubly excited states have been studied often in H_2 [2–5], their study in, e.g., N_2 is simpler because in such a molecule they are more separated in energy and the atomic asymptotic states are not highly degenerate. For the photodissociation of N_2 in the energy range within 10 eV above the first ionization energy, there is a complex series of processes which has yet to be fully unraveled (see Fig. 1). It is possible to have direct dissociation, autoionization and dissociation, or predissociation of bound states by repulsive states. Previous experiments involving the dissociation of doubly excited states in N_2 have involved either the measurement of the fluorescence intensity from excited fragments [9,12] as a function of incident photon energy or the detection of neutral or ionic fragments [13]. These measurements have been able to identify the presence of predissociating states though they are less successful at identifying the mediating repulsive states associated with this predissociation or the presence of any direct dissociation.

In this Rapid Communication we show how the measurement of circular fluorescence polarization can provide information about dissociation dynamics. The development of a complete quantum mechanical treatment of diatomic dissociation [14,15] provides us with the basis for using the measurement of photofragment polarization to probe the angular momentum state of the excited molecule and the dissociation dynamics. While previous work on other molecules has used circular polarization analysis to examine the dissociation process, all such studies have involved the polarization of nonfluorescing electronic ground states [16–20]. We report here the measurement of the circular polarization, P_3, of light

emitted directly from excited neutral atoms created in the photofragmentation of diatomic molecules.

When a molecule is excited by a photon, the number of possible final excited states is limited by dipole selection rules ($\Delta\Lambda = 0, \pm 1$ and $\Delta S = 0$) so that only states of $^1\Sigma_u^+$ and $^1\Pi_u$ symmetry can be populated directly from a $^1\Sigma_g^+$ ground state, though spin conservation rules are not strict for heavy molecules. If circularly polarized photolysis radiation is used, then orientation (differences in the $+M$ and $-M$ populations yielding a magnetic dipole) of the excited molecular state is possible. Orientation of the photofragments along the incident beam direction, averaged over all recoil directions, can only be produced with circularly polarized photolysis radiation when a perpendicular transition ($\Delta\Lambda = \pm 1$) occurs [14,15]. Thus, the orientation of N_2 excited from the $^1\Sigma_g^+$ state, as inferred from nonzero values of fluorescence P_3 from a photofragment, must involve the initial excitation of a $^1\Pi_u$ molecular state. This can be either a directly dissociating doubly excited state or one which is predissociated by a state of either Σ or Π symmetry. Our measurements have yielded insight into the nature of both predissociating and promptly dissociating states, allowing us to unambiguously identify one channel for dissociation of N_2 with an excited $N[3p(^4P^0)]$ state: direct excitation of a non-Rydberg doubly excited resonance (NRDER) leading promptly to the excited-state photofragments. The NRDER states are essentially resonances in the photoionization continuum and can either autoionize or dissociate into neutral fragments with at least one of the neutral fragments in an excited state [9,10].

In our experiment, we observe combined 818.5- and 818.8-nm fluorescence from N I $2p^2\,3p(^4P^0)$ states produced in the reaction

$$\gamma + N_2 \to N_2{}^{**} \to N[3p(^4P^0)] + N[2p^3(^4S)]. \quad (1)$$
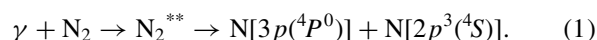
In the range of incident photon energies we studied, 21–26 eV, these states are produced by (a) the predissociation
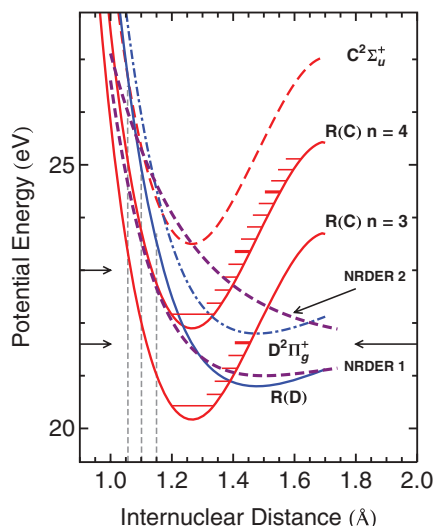
FIG. 1. (Color) Potential energy diagram for N_2 and N_2^+ showing from top down at the right: C $^2\Sigma_u^+$ [6]; the Rydberg series $R(C)$ $n = 4$ [7]; $R(C)$ $n = 3$; NRDER 2 that predissociates the $R(C)$ $n = 4$ and $n = 5$ states to produce N* $4P$ states; D $^2\Pi_g^+$ [8]; NRDER 1 which is directly excited and promptly dissociates to produce N* $4P$ states; the Rydberg series $R(D)$ $n = 4$ state [9]. The arrow at the right indicates the production threshold for N* $4P$ states, and the two arrows at the left indicate the energies of the intensity feature maxima at 21.6 and 23 eV (see text). The NRDER and R(x) curves are based on the analyses of Refs. [7,9,10] and on quantitative considerations discussed below. The dashed gray vertical lines show the center and bounds of the Franck-Condon region [11].

by repulsive NRDERs of the doubly excited Rydberg series $R(C)$ ($^1\Sigma_u^+$) that converge to the C $^2\Sigma_u^+$ states of N_2^+ [9], and (b) the direct excitation and dissociation of NRDERs. Our measurements were performed on the high-resolution Atomic, Molecular and Optical Physics undulator beam line 10.0.1.2 of the Advanced Light Source (ALS) at the Lawrence Berkeley National Laboratory. A schematic diagram of the apparatus is shown in Fig. 2. A grazing-incidence spherical-grating monochromator was used to scan the incident photon energy

for both intensity and polarization measurements. Previous measurements [3] indicate that in this energy range there is contamination of our beam due to third-order on-axis harmonics of about 10%. The light from the monochromator had a linear polarization in the horizontal plane greater than 99%. A four-reflector quarter-wave retarder was inserted to create circularly polarized VUV radiation [21]. The linear polarization P_1^i of the incoming light was measured using a Au reflector polarization analyzer which could be rotated azimuthally [22]. Circular polarization of the beam, P_3^i, was inferred by measuring its linear polarization and using the following relationship:

$$P_3^i = \left(1 - P_1^{i\,2}\right)^{1/2}. \tag{2}$$

The circular polarization of the beam varied between 99% and at least 99.99% over the energy range of interest.

A maximum flux of $\sim 3 \times 10^{13}$ photons/s was available at 25 eV with an unmodified linearly polarized beam as used in the total intensity measurements. However, the flux is reduced by at least a factor of 100 by the retarder. The incident photon flux was monitored using a NIST calibrated photodiode (IRD AXUV100). The polarized light was collimated to a beam spot size of ~ 0.5 mm and then intersected an effusive target of N_2 gas at room temperature. The target gas purity was 99.9995% as specified by the supplier. The chamber pressure was kept between 9×10^{-6} and 2×10^{-5} Torr corresponding to a pressure in the interaction region between 20 μTorr and 5 mTorr.

The collision region was observed by photon detectors in two different configurations. The photon detector axis for the intensity measurements made a polar angle of 35.3° relative to the incident photon axis. This detector was in the plane defined by the electric field of the incident photons and their propagation axis when linearly polarized light was used. The photon detector comprised a $f/1.9$ fused-silica collection lens, a polarization analyzer, an interference filter to select the observed atomic transitions, and a lens to refocus the collimated light onto the photocathode of a photomultiplier tube (Hamamatsu R943-02). The P_3 measurements used a detector with its axis at 30° to the incident beam direction. The optical polarimeter used a rotating quarter-wave retarder followed by a fixed linear polarizer. An interference filter which had a center wavelength of 818.7 nm selected two N I lines, the $3p$ $^4P_{3/2}^o \rightarrow 3s$ $^4P_{1/2}$ transition at 818.8 nm and the $3p$ $^4P_{5/2}^o \rightarrow 3s$ $^4P_{3/2}$ transition at 818.5 nm. The detection of these of lines is free from any molecular contamination [9].

The photon emission axis used in the intensity measurements was at the "magic" angle of 54.7° with respect to the incident beam polarization axis. Thus the measured intensity was proportional to the excitation cross section and independent of the polarization of the fluorescent emission; no polarization analyzer was used in these experiments. The incident beam energy had an energy resolution of 40 meV and was scanned in 10-meV steps. Measurements of P_3 were obtained by rotating the retarder fast axis in the polarimeter and measuring the variation in the detected light intensity [23]. For these experiments, which used circularly polarized incident light, the energy was scanned in 0.1-eV steps and the photons had an energy resolution less than 50 meV. In all cases the full detector photon counting rate was corrected for dark counts and beam-related background and normalized to the incident
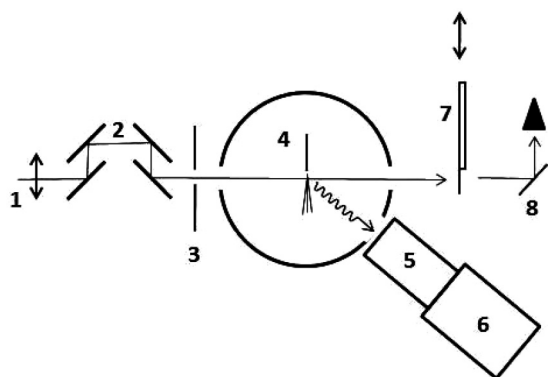

FIG. 2. Apparatus schematic showing (1) incident photon beam from ALS synchrotron, linearly polarized in the plane of the diagram, (2) insertable four-reflection quarter-wave retarder, (3) beam-defining aperture, (4) effusive N_2 target, (5) optical polarimeter at the magic angle, (6) photon-counting photomultiplier tube, (7) photodiode for incident photon flux normalization, and (8) linear photon polarimeter.
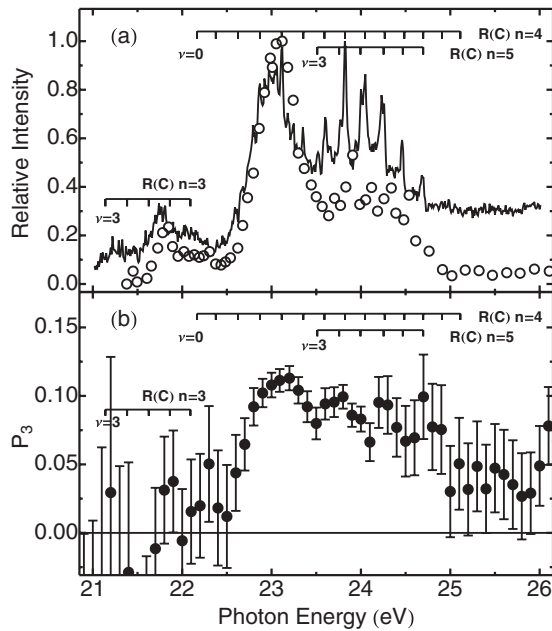
FIG. 3. (a) 818-nm intensity data: The solid black line is the present intensity data, and the open circles are the experimental results of Erman *et al.* [9]. The position of the vibrational structure is based on the assignments of Codling [7]. (b) The solid circles are the present circular polarization P_3 data.

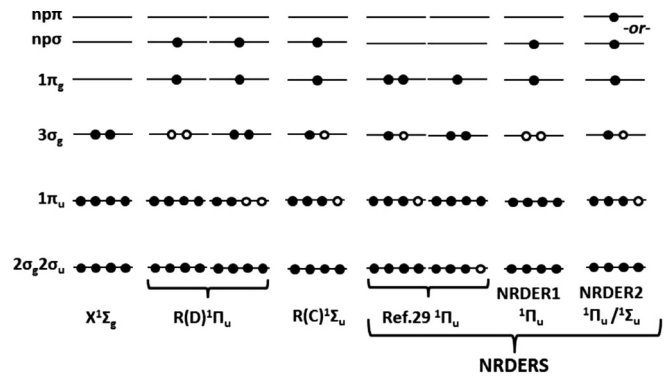FIG. 4. Configurations of various neutral N_2 molecular states including the ground state (X), Rydberg states converging to the ions N_2^+ C [$R(C)$] and D [$R(D)$], and NRDER states discussed in various references (see text). The G $1\sigma_g 1\sigma_u$ orbitals are filled for all of these states and are not shown. In the cases where two configurations have been suggested for a given state [$R(D)$ [30] and the NRDER proposed by Wendin [12,29]] both are shown, with the primary configuration at the left.

beam flux and gas target pressure. Our results have also been corrected for deviations from ideal quarter-wave retardance and the extinction coefficient of the polarizers. The reported P_3 values have been calculated as a moving weighted average of P_3 for three consecutive energies.

Since predissociation occurs over a period that is shorter than 25 fs [24], little hyperfine or rotational depolarization occurs in the excited molecular state. However, the polarization of the light emitted from the neutral fragments is decreased due to hyperfine effects [25–27]. The hyperfine splitting of the $^4P^o_{5/2}$ state is approximately 25 MHz and that of the $^4P^o_{3/2}$ state is approximately 110 MHz [28] with lifetimes of 116 and 79 ns, respectively, so the polarization of the detected fluorescence is reduced between 15% and 30%. The P_3 data include the effects of hyperfine depolarization.

The fluorescent intensity spectrum is shown in Fig. 3(a). It has several features, including a small peak at 21.6 eV which is about 0.4 eV wide, and a much more intense, broad peak at 23 eV. Superimposed on the broader underlying peak between 22.5 and 25 eV is vibrational structure associated with the $R(C)$ state. The circular polarization P_3 shown in Fig. 3(b) has definite nonzero values above 22.5 eV and is consistent with zero elsewhere.

In terms of the broad feature between 22.5 and 25 eV, we observe a much better defined vibrational structure with different relative intensities when compared with Erman *et al.* [9] due to the improved resolution of the present measurement and possibly the selection of only two ($J = 1/2$ and $J = 3/2$) of the four possible lines emitted from the ^4P fine-structure states. This vibrational structure is consistent with the excitation of the $1\pi_u^3 3\sigma_g 1\pi_g ns\sigma$ $\left(^1\Sigma_u^+\right)$ $R(C)$ $n = 4$ and $n = 5$ states (see Fig. 4) [7]. The vibrational assignments

shown in Fig. 3 for the $n = 4$ and $n = 5$ $R(C)$ states are taken from Codling; our data was shifted by 10 meV to match these energies. We note that with our present energy resolution of 40 meV we are able to distinguish features in both the $R(C)$ $n = 4$ and $n = 5$ states, e.g., the $n = 4$, $\nu = 8$ and the $n = 5$, $\nu = 5$ states, which are separated by 50 meV [7]. The existence of these vibrational state features indicates that one dissociation channel involves direct production of the $n = 4$ and $n = 5$ $R(C)$ states which are then predissociated by NRDERS [9,12,13,29]. The NRDERS proposed by Wendin [29] and Erman *et al.* [9] [the latter specifically for predissociation of the $R(C)$ states, "NRDER2"] and shown in Fig. 4 seem to be the most likely candidates to play this role, given the similarity of their configurations and that of the $R(C)$ state.

This predissociative mechanism, however, must be associated with $P_3 = 0$ because the $R(C)$ states have Σ symmetry. Thus our circular polarization data require a second dissociative mechanism: the direct production and dissociation of NRDERs with $^1\Pi_u$ symmetry. The polarization P_3 is reduced from its maximum because of increasingly important contributions from the predissociative $R(C)$ channels to N I production as the incident photon energy increases above 23 eV. Both Ukai *et al.* [12] and Erman *et al.* [10] have suggested that the prominent peak at 23.5 eV in the visible fluorescence observed by Ukai *et al.*, and which corresponds to our feature at this energy, is due to direct $^1\Pi_u$ NRDER production followed by dissociation. Hikoska *et al.* [13] attributes a similar broad feature in N atom neutral production to the same process. The broad featureless nature of these peaks at 23.5 eV certainly implies that rapid dissociation of a short-lived doubly excited state is responsible for them. However, Ukai *et al.* [12] and Hikosaka *et al.* [13] suggest that the $^1\Pi_u$ doubly excited state of Wendin [29] (indicated as "Ref. [29]" in Fig. 4) is responsible for this feature, whereas Erman *et al.* [10] propose a higher-lying NRDER (NRDER1; Fig. 4).

Given its appropriate calculated energy in the N_2 Franck-Condon region (23.6 eV), we suggest that the second lowest $^1\Pi_u$ state of Erman *et al.* [10] is the best candidate for

this NRDER (NRDER1 in Fig. 4). As mentioned above, Erman *et al.* [9] only discuss this feature in terms of predissociative processes involving NRDER2 (Fig. 4). Our data provide unambiguous evidence for direct population through an optically allowed two-electron NRDER with $^1\Pi_u$ symmetry leading to prompt dissociation.

With regard to the feature at 21.6 eV we can say two things. First, P_3 in this energy range is consistent with zero. This implies that either a directly excited NRDER or a predissociated initial state responsible for this feature must be of Σ symmetry. Second, we observe no discernible vibrational structure in the intensity spectrum. Features in other spectra in the vicinity of 21.6 eV have been suggested to be caused by the predissociation of $R(D)$ $^1\Pi_u$ states [9,30,31]. Our polarization data do not support this. Moreover, there is indirect evidence that the $R(D)$ designation is wrong. First, the NRDERs suggested by Erman *et al.* [9] as being responsible for coupling the $R(D)$ state to the dissociative continuum (NRDER2; Figs. 1 and 4) would almost certainly be more strongly coupled to an $R(C)$ configuration than one associated with $R(D)$, as can be seen in Fig. 4. Second, the energy of the $R(C)$ $n = 3$, $v = 0$ level, as inferred from the established quantum defect for the $R(C)$ states [7,30], occurs at 20.43 eV. Indeed, the threshold for $R(C)$ Franck-Condon excitation as seen in Fig. 1 indicates an onset for this feature above 21 eV, in agreement with our intensity spectrum. The $R(C)$ assignation is supported by Ukai *et al.* [12] (although this is questioned by Erman *et al.* [31]). Referring again to Fig. 1 it is apparent that excitation of an $R(D)$ state by a Franck-Condon transition is forbidden. While it has been pointed out that configuration mixing and σ_g^{-1} shape resonances are responsible for significant deviations from Franck-Condon behavior [7,10,32], no calculations of which we are aware support such an extreme breakdown of the Franck-Condon approximation in this situation.

Our failure to observe vibrational structure in the 21.6-eV feature is consistent with the data of Ukai *et al.* [12], Wu *et al.* [30], and Erman *et al.* [9]. Erman *et al.* [31], who studied VUV fluorescence spectra, do see hints of structure at this energy. A recent report by Lo *et al.* [33], who also study VUV fluorescence spectra (but with roughly a factor of 100 better resolution than that of Erman *et al.* [31]), see an irregular structure superimposed on a broader feature between 21.5 and 21.9 eV, but with no consistent spacings to suggest vibrational structure associated with either an $R(C)$ or an $R(D)$ state. One can only say that the lack of obvious structure in most data sets suggests an alternate possibility: that this feature is due not to a predissociative channel but rather the direct production of an optically allowed Σ-symmetry NRDER, possibly of the type identified by Sannes and Veseth [34].

In summary, we have measured the total fluorescent intensity and circular polarization of light emitted from the $3p$ $^4P^o$ to $3s$ ^4P transitions of excited neutral nitrogen created in the photofragmentation of the N_2 molecule by circularly polarized light between 21 and 26 eV. Vibrational structure in the total intensity measurements above 22.5 eV corresponding to the doubly excited Rydberg series $R(C)$ that converge to the C $^2\Sigma_u^+$ states of N_2^+ provide a clear indication of predissociation of the excited molecular $R(C)$ states by NRDERs. These $R(C)$ states have $^1\Sigma_u^+$ symmetry. However, the observation of orientation via the measurement of nonzero P_3 values in the energy region where this predissociation occurs indicates that direct excitation of a $^1\Pi_u$ NRDER state must also occur. Thus while the total intensity measurements involve the predissociating $R(C)$ states, the P_3 measurements unambiguously reveal the primary influence of directly excited NRDERs. The polarization analysis also suggests the interpretation of the feature in the total intensity measurements near 21.6 eV as being due to excitation of a state with Σ symmetry since a zero P_3 in the vicinity of 21.6 eV rules out the possibility of $R(D)$ $^1\Pi_u^+$ predissociation. This supports the assignment by Ukai *et al.* [12] of this feature as an $R(C)$ $^1\Sigma_u^-$ predissociated state. It could also result from direct excitation of a directly dissociating state with Σ symmetry.

[1] R. L. Platzman, Radiat. Res. **17**, 419 (1962).

[2] M. Glass-Maujean, R. Kneip, E. Flemming, and H. Schmoranzer, J. Phys. B **38**, 2871 (2005).

[3] J. R. Machacek, V. M. Andrianarijaona, J. E. Furst, A. L. D. Kilcoyne, A. L. Landers, E. T. Litaker, K. W. McLaughlin, and T. J. Gay, J. Phys. B **44**, 045201 (2011).

[4] Y. Hatano, Phys. Rep. **313**, 109 (1999).

[5] J. Fernandez and F. Martin, J. Phys. B **34**, 4141 (2001).

[6] S. R. Langhoff and C. W. Bauschlicher, J. Chem. Phys. **88**, 329 (1988).

[7] K. Codling, Astrophys. J. **143**, 552 (1966).

[8] P. Baltzer, M. Larsson, L. Karlsson, B. Wannberg, and M. Carlsson Göthe, Phys. Rev. A **46**, 5545 (1992).

[9] P. Erman, A. Karawajczyk, E. Rachlew-Källne, J. Rius i Riu, M. Stankiewicz, K. Yoshiki Franzén, and L. Veseth, Phys. Rev. A **60**, 426 (1999).

[10] P. Erman, A. Karawajczyk, U. Köble, E. Rachlew, K. Yoshiki Franzén, and L. Veseth, Phys. Rev. Lett. **76**, 4136 (1996).

[11] F. R. Gilmore, J. Quant. Spectrosc. Radiat. Transfer **5**, 369 (1965).

[12] M. Ukai, K. Kameta, N. Kouchi, Y. Hatano, and K. Tanaka, Phys. Rev. A **46**, 7019 (1992).

[13] Y. Hikosaka, P. Lablanquie, M. Ahmad, F. Penent, J. H. D. Eland, and R. I. Hall, J. Phys. B **37**, 283 (2004).

[14] J. A. Beswick, M. Glass-Maujean, and O. Roncero, J. Chem. Phys. **96**, 7514 (1992).

[15] L. D. A. Siebbeles, M. Glass-Maujean, O. S. Vasyutinskii, J. A. Beswick, and O. Roncero, J. Chem. Phys. **100**, 3610 (1994).

[16] O. S. Vasyutinskii, Sov. Phys. JETP **54**, 855 (1981).

[17] T. P. Rakitzis, P. C. Samartzis, R. L. Toomes, T. N. Kitsopoulos, A. Brown, G. G. Balint-Kurti, O. S. Vasyutinskii, and J. A. Beswick, Science **300**, 1936 (2003).

[18] E. Hasselbrink, J. R. Waldeck, and R. N. Zare, Chem. Phys. **126**, 191 (1988).

[19] Z. H. Kim, A. J. Alexander, S. A. Kandel, T. P. Rakitzis, and R. N. Zare, Faraday Discuss. **113**, 27 (1999).

[20] A. G. Smolin, O. S. Vasyutinskii, O. P. J. Vieuxmaire, M. N. R. Ashfold, G. G. Balint-Kurti, and A. J. Orr-Ewing, J. Chem. Phys. **124**, 094305 (2006).

[21] T. Döhring, G. Schonhense, and U. Heinzmann, Meas. Sci. Technol. **3**, 91 (1992).

[22] K. Rabinovitch, L. R. Canfield, and R. P. Madden, Appl. Opt. **4**, 1005 (1965).

[23] H. G. Berry, G. Gabrielse, and A. E. Livingston, Appl. Opt. **16**, 3200 (1977).

[24] D. Strasser, L. H. Haber, B. Doughty, and S. R. Leone, Mol. Phys. **106**, 275 (2008).

[25] U. Fano and J. H. Macek, Rev. Mod. Phys. **45**, 553 (1973).

[26] A. J. Orr-Ewing and R. N. Zare, Annu. Rev. Phys. Chem. **45**, 315 (1994).

[27] K. Blum, *Density Matrix Theory and Applications*, 2nd ed. (Plenum, New York, 1996).

[28] P. Cangiano, M. de Angelis, L. Gianfrani, G. Pesce, and A. Sasso, Phys. Rev. A **50**, 1082 (1994).

[29] G. Wendin, Int. J. Quantum Chem. **16**, 659 (1979).

[30] C. Y. R. Wu, L. C. Lee, and D. L. Judge, J. Chem. Phys. **80**, 4682 (1984).

[31] P. Erman, A. Karawajczyk, E. Rachlew-Kallne, S. L. Sorensen, C. Stromholm, and M. Kirm, J. Phys. B **26**, 4483 (1993).

[32] J. Rius i Riu, A. Karawajczyk, M. Stankiewicz, K. Yoshiki Franzén, P. Winiarczyk, and L. Veseth, Chem. Phys. Lett. **338**, 285 (2001).

[33] J. I. Lo, M. H. Tsai, H. S. Fung, Y. J. Chen, C. C. Chu, T. S. Yih, Y. Y. Lee, C. Y. R. Wu, and D. L. Judge, J. Chem. Phys. **137**, 054315 (2012).

[34] P. Sannes and L. Veseth, Phys. Rev. A **56**, 2893 (1997).